buildings

MDPI

Article

Experimental Research on the Seismic Behavior of Reinforced Concrete Column–Beam Joints Connected by Π-Shaped Steel Plates

Jian Wu [1], Ying Jiang [1], Jian Zhou [2], Liangjie Hu [1], Jianhui Wang [1] and Weigao Ding [3,*]

[1] Shaanxi Key Laboratory of Safety and Durability of Concrete Structures, Xijing University, Xi'an 710123, China; wujian2085@126.com (J.W.)
[2] Northwest Engineering Corporation Limited, Xi'an 710065, China
[3] School of Infrastructure Engineering, Dalian University of Technology, Dalian 116024, China
* Correspondence: 745571908@mail.dlut.edu.cn

Abstract: The mechanical performance of existing buildings degrades over time, and even if the mechanical performance meets the requirements, some buildings will have new usage needs, necessitating the reinforcement and renovation of buildings. Therefore, this paper conducted experimental research on the reinforcement and renovation of reinforced concrete joints that could simultaneously meet the requirements for seismic performance and new usage needs. Firstly, the reinforced concrete columns are produced, and the treatment of the wrapped steel plate is conducted. Then, the Π-shaped steel plate is welded onto the wrapped steel of the column, and the longitudinal bars of the beam and the Π-shaped steel plate are connected through the weld seam. Finally, we proceed with pouring the concrete for the beam and wrapping the beam with the steel plate. After the completion of specimen production, a cyclic loading test is conducted to compare and analyze the hysteresis curve, ductility, stiffness degradation, and energy dissipation of the new specimen type and cast-in-place specimen. The steel plate thickness, including the wrapped steel of the beam and the Π-shaped steel plate, is designed as a variable for the experiment. The results indicate that the seismic properties of the specimen are effectively improved after reinforcement with a steel plate. At the same time, the seismic performance of the specimen improves with an increase in the thickness of the steel plate wrapping the beam, while the impact of the Π-shaped steel plate is relatively minimal. The research results show that compared with the cast-in-place specimen, the reinforcement and renovation method proposed in this paper can significantly improve the seismic performance of the specimen and can help promote the development of urban reinforcement and renovation work.

Keywords: reinforced concrete joints; reinforcement and renovation; Π-shaped steel plate; experimental study; seismic performance

Academic Editors: Haibo Jiang, Renda Zhao, Yunchao Tang, Xiaohong Zheng and Fangwen Wu

Received: 30 December 2024
Revised: 20 January 2025
Accepted: 22 January 2025
Published: 23 January 2025

Citation: Wu, J.; Jiang, Y.; Zhou, J.; Hu, L.; Wang, J.; Ding, W. Experimental Research on the Seismic Behavior of Reinforced Concrete Column–Beam Joints Connected by Π-Shaped Steel Plates. *Buildings* **2025**, *15*, 349. https://doi.org/10.3390/buildings15030349

1. Introduction

The reinforced concrete (RC) frame, as the most common form of concrete structure, is widely used all over the world for its benefits, including large spaces and large spans. In China, a lot of RC structures, after long periods of use, are subjected to external loads such as earthquakes, wind, and applied loads, as well as their own gravity loads. The stiffness and strength of the materials, components, and structures gradually degrade, and their bearing capacity and seismic performance decrease, no longer meeting the requirements for

safe use [1–3]. At the same time, even if the structure can still meet the safety requirements, the former design standards can no longer meet the usage requirements [4,5]. In such cases, it is necessary to reinforce and renovate the existing RC frame structures. As an important component of concrete frame structures, the mechanical properties of the joints directly affect the safety of the structure. These observations indicate that the study of the reinforcement and renovation of the joint is required.

At present, reinforcement treatment of RC frame joints is being gradually implemented. The current joint reinforcement methods mainly include the enlarging section method, fiber reinforcement method, and wrapped steel reinforcement method [6–8]. The enlarging section method affects the usage space of the structure and involves wet construction, while fiber materials have the characteristic of only being able to withstand tension but not compression, limiting their applicability. Under the premise of guaranteeing the reinforcement effect, the wrapped steel reinforcement method can effectively reduce the impact on the normal life of residents and use space. Therefore, the wrapped steel reinforcement method is a joint reinforcement form worth promoting. Li et al. [9] investigated the performance of a steel beam–column joint wrapped with a steel tubular and found that the ductility of this type of specimen is better than that of ordinary specimens. Zhou et al. [10] studied the seismic performance of L-shape joint specimens with beams wrapped with steel. The results showed that the failure mode was bending failure, and the seismic properties of this type of specimen were better than the specimen wrapped with a steel beam. Lee et al. [11] studied the seismic behavior of a joint comprising a concrete-filled tubular column and a concrete beam. Their findings indicated that the joint met the criteria for strength and energy dissipation, albeit with low rigidity. Derakhshesh et al. [12] introduced a joint formed using a steel beam and a concrete-encased column, and the connection of the beam and the column was realized through a flange plate. The results indicated that the main resistant elements were flange plate, and the performance of the specimen was improved. Liu et al. [13] introduced the properties of an L-shaped concrete column wrapped with steel and found that the wrapped steel could effectively restrain specimen buckling and improve the ultimate bearing capacity and stiffness. Fang et al. [14] analyzed the properties of an encased concrete column and found that its initial stiffness and compressive capacity were effectively improved. Chen et al. [15] investigated the flexural performance of the beam, which was formed using encased steel and different types of concrete. The results indicated that the bearing capacity of the new type of specimen is 24.6% higher than an ordinary RC beam. Cai et al. [16] investigated the seismic performance of a beam–column joint strengthened by steel haunches and a bolted steel plate and found that the mechanical properties were significantly improved. Zhang et al. [17] studied the flexural behavior of the beam encased in a U-shape steel plate. The results indicate that the strengthened beam had a better ductility coefficient. These research results indicate that steel reinforcement can effectively improve the mechanical properties of structures or their components. However, there is currently relatively little research on steel reinforcement methods for existing RC buildings. Therefore, this paper adopts the steel reinforcement method to treat joints and study its application in engineering reinforcement.

At the same time, the renovation of buildings can eliminate safety hazards and meet the requirements of new regulations and functions. Nguyen et al. [18] designed a beam-column joint whose RC beam was welded to the exposed reinforcement of the column, and they found that the mechanical performance of this type of specimen was poorer than that of a precast one. Ertas et al. [19] analyzed the performance of welded, bolted, post cast-integral, and standard joint specimens. The results indicated that bolted connections not only exhibited favorable and efficient characteristics during construction but also demonstrated optimal performance in indicators such as strength, ductility, and energy

dissipation capacity. Choi et al. [20] investigated a new type of joint consisting of a column wrapped with a square tube and a beam using cast-in-situ concrete. It could be concluded that the plastic hinge on the beam controls the failure of the specimen, and the joint strength is 1.15 times that of the cast-in-place RC structure. Ali et al. [21] studied the bending behavior of beam–column joints made of mixed concrete, and they found that compared to the standard joint, the usage of mixed concrete in different regions would improve the bearing capacity, initial crack load, and ductility by about 8–32%, 20–60%, and 6–14%, respectively. Kurosawa et al. [22] studied a prefabricated prestressed concrete frame equipped with lightweight compression joints. The experimental data showed that, compared to the RC frame structure, this type of structure exhibited better damage tolerance characteristics in crack control and residual displacement. Zhang et al. [23] introduced a joint consisting of a circular steel pipe column, a RC beam, and a flange cover plate (FCP), and they found that the seismic properties were improved and the plastic deformation was concentrated on the easily replaceable FCP, ensuring that structural components did not undergo plastic damage. Cao et al. [24] investigated the mechanical properties of a specimen consisting of a concrete-filled steel tube (CFST) column, a steel beam, and a Π-shape connector. The results demonstrated that enhancing the Π-shaped connector and incorporating a web plate could augment the properties of the specimen. Zeinab et al. [25] improved the beam–column connection by adding flange covers at the top and bottom of the beam. The results indicated that the hysteresis curve of the specimen had good compatibility, and the yielding of the beam occurred on the outer side of the cover plate. Joshi et al. [26] investigated the performance of joints consisting of a RC column and a steel beam. The results showed that the deformation of the shear plate embedded in the profile had a significant impact on the overall performance of the specimen. Huang et al. [27] investigated the properties of a beam–column joint connected by a replaceable friction plastic hinge, and they found that the relatively low yield load diminished the energy dissipation capacity of the specimen during the initial phase of loading. These research results indicate that an effective connection between components can be achieved through effective treatment methods, but these connection methods often have disadvantages such as high cost, complex construction, and significant damage to the existing components. Therefore, this paper chooses to wrap steel plates around columns and use Π-shaped steel plates to connect the beams and columns together.

In this paper, a new type of reinforced concrete joint is introduced to promote the development of reinforcement and renovation technology. Four joints are designed to investigate the performance of the specimen, three of which are new types of joints and one is a cast-in situ RC specimen. The former specimen consists of a RC column, a RC beam, and a Π-shaped connector. The column and beam are encased in a steel plate, and the wrapped steel of the beam and Π-shaped connector are both welded onto the wrapped steel of the column, while the longitudinal bars of the beam are welded onto the connector. Through cyclic loading, the hysteretic curve, skeleton curve, ductility, rigidity, and energy dissipation capacity of the specimen are obtained. The experimental results aid in the evaluation of the impact of the thickness of the steel plate wrapping the beam and the Π-shaped steel plates on the mechanical properties of the specimen.

2. Designing and Testing

2.1. Designing the Specimens

In this paper, four specimens are designed, including three beam–column joints connected by a Π-shaped steel plate (new type of joint) and one cast-in-place RC joint (standard joint). The new types of joints are numbered JGJ1–JGJ3, and the standard joint is denoted by BZJ (Figure 1).

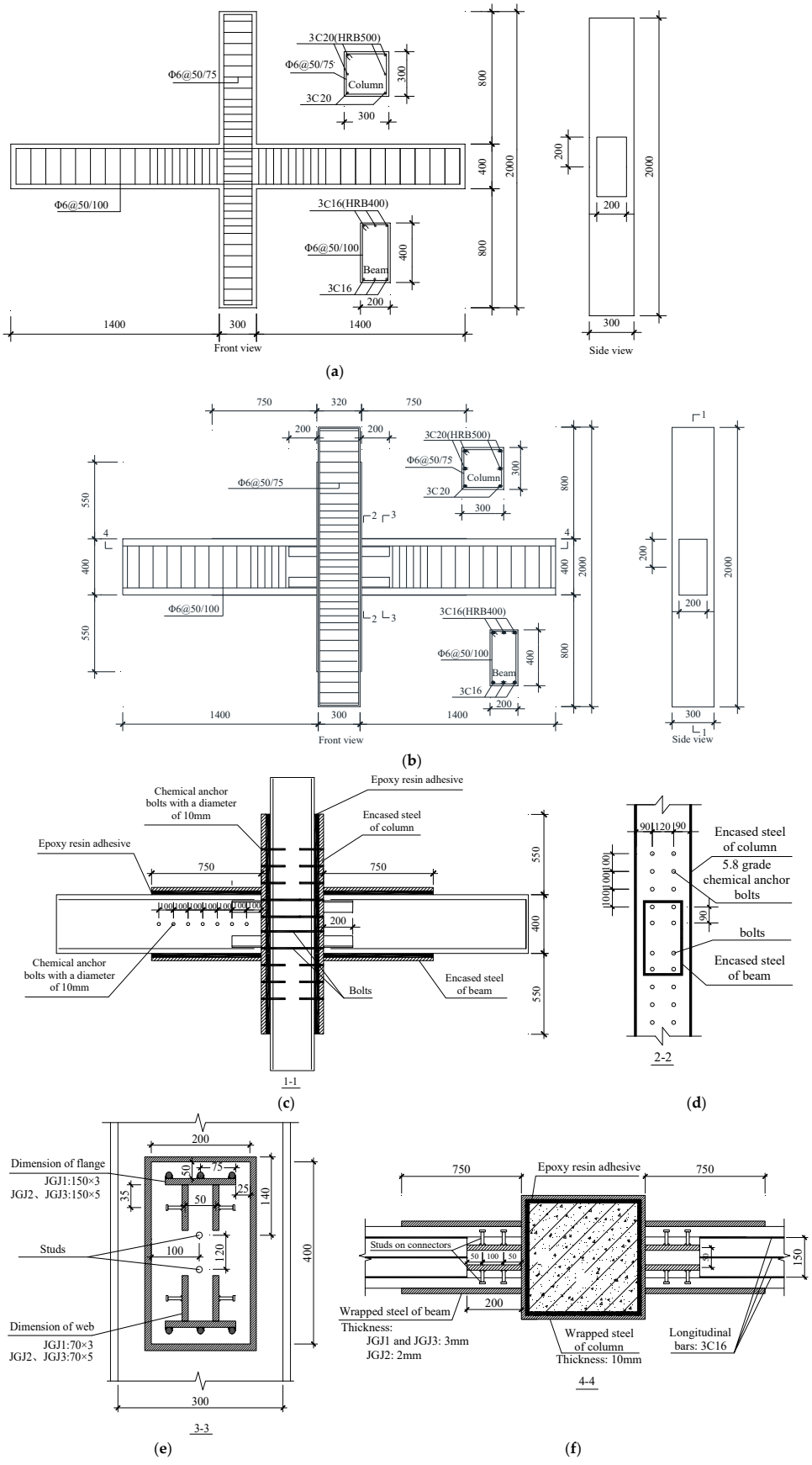

Figure 1. Design scheme: (**a**) BZJ; (**b**) new type of specimen; (**c**) 1-1 sectional view of the new type of specimen; (**d**) 2-2 sectional view of the new type of specimen; (**e**) 3-3 sectional view of the new type of specimen; (**f**) 4-4 sectional view of the new type of specimen.

The design condition of BZJ is given in Figure 1a. The length of the beam is 3100 mm; the sectional dimension is width × height = 200 mm × 400 mm; and the longitudinal reinforcement is 3C16, which is symmetrically arranged. The length of the column is 2000 mm; the sectional dimension is length × height = 300 mm × 300 mm; and the longitudinal reinforcement on one side is 3C20 which is symmetrically arranged. The beam and column near the core area represent the stirrup encryption area, and the length is 500 mm. The thickness of the concrete cover is 10 mm.

The dimensions and materials of the new types of joints are the same as those used for the standard one (Figure 1b). The difference is that after pouring the concrete for the column and completing the maintenance of the new type of joint, the column would be encased in a steel plate. Then, the Π-shaped steel plate is welded in the middle of the wrapped steel on both sides of the column and welded with the longitudinal reinforcement of the beam. Finally, the concrete is poured, and the steel plate is wrapped and welded with that of the column.

Considering the design concept of strong columns and weak beams in the frame structure, 10 mm thick steel plates are selected for the columns and 3 mm thick steel plates are selected for the beams in the wrapped steel design of the specimens. It should be noted that if the steel thickness of the beam is a smaller value, the quality of the welding cannot be guaranteed, so the thickness is set to 3 mm. At the same time, taking into account that the mechanical properties of the beam after being wrapped in steel will change, through preliminary finite element analysis, this paper sets the length of the beam wrapped in steel to 750 mm. At this time, the part of the beam that is not wrapped in steel can resist the bending moment and shear force it receives. That is, if the strength of the steel plate is too high and the requirements for the specimen support device are too high. Therefore, from the perspective of test safety, the steel strength selected in this paper is Q345.

The specific design points are as follows:

1. Treatment of wrapped steel. In the fabrication process of the new types of joints, the epoxy resin adhesive is first applied on the surface of the concrete before the wrapping of steel to ensure the bonding effect between steel and concrete. Then, chemical anchor bolts are placed on the outer side of the joint, as shown in Figure 1c. The chemical anchor bolts used for the wrapped steel of the beam are grade 5.8, with a diameter of 8 mm and a spacing of 100 mm. The chemical anchor bolts used in the encased steel of the column are grade 5.8, with a diameter of 10 mm and a spacing of 100 mm. The chemical anchor bolts used in this paper are produced by Daze Fastener Manufacturing Co., Ltd. in Handan City, Hebei Province, China. Based on the finite element analysis results, the chemical anchor bolts used in the beams and columns ensure that there is no slip or vertical separation between the steel plate and the concrete. At the same time, considering the complexity of the force at the intersection of the beam and the column, four rows of bolts are arranged on the side of the column, two bolts for each row, as shown in Figure 1d. The quantity and arrangement of the bolts are determined based on the specifications of Chinese standard GB 50205-2001 [28] and the influence of the location of the connector, which ultimately inform the layout chosen for this paper.
2. Design points for the Π-shaped steel plates (connectors). The connector consists of a flange and two webs. The width of the flange is 150 mm and the length along the length direction of the beam is 200 mm. The dimensions of the web are 70 mm × 200 mm. The thicknesses of the flange and the web differ across different specimens. The thickness of the flange and web of JGJ1 and JGJ2/3 are 3 mm and 5 mm, respectively. The design condition of the steel plate is given in Table 1. The center spacing of the web is 50 mm, the length of the upper edge of the flange from

the lower edge of the wrapped steel of the beam is 50 mm, and the outer edge of the flange is 25 mm from the encased steel of the beam on both sides. The steel bars of the beam are welded onto the outer side of the flange, and there are no stirrups in the range of the connector. The construction of the connector is given in Figure 1e,f.

Table 1. Properties of the steel plate.

Number	Length of Wrapped Steel of Column (mm)	Thickness of Wrapped Steel of Column (mm)	Length of Wrapped Steel of Beam (mm)	Thickness of Wrapped Steel of Beam (mm)	Thickness of the Connector (mm)	Types of Steel
BZJ	-	-	-	-	-	-
JGJ-1	1500	10	750	3	3	Q345
JGJ-2	1500	10	750	2	5	Q345
JGJ-3	1500	10	750	3	5	Q345

3. The connection treatment between the concrete and steel plate. Two studs are arranged on the wrapped steel around the column with a spacing of 120 mm and 100 mm from the outer edge of the beam (Figure 1e). Two studs are arranged on each of the two webs of the connector with a spacing of 100 mm, as shown in Figure 2.

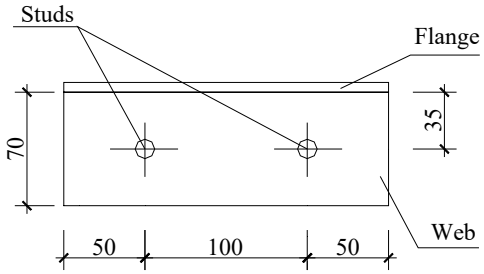

Figure 2. Arrangement of studs.

2.2. Properties of the Materials

2.2.1. Concrete

The concrete used for the specimens in the fabrication process is poured in 3 batches; the 1st batch of concrete is poured for the column of all specimens (C50-1), the 2nd batch of concrete is poured for the beam of BZJ (C40-1), and the 3rd batch of concrete is poured for the beam of JGJ1–JGJ3 (C40-2). The designed concrete strength grades of the beam and column are C40 and C50, respectively. Three cubic specimens (150 mm × 150 mm × 150 mm) are reserved for each batch to determine the strength of the concrete. According to the specifications of Chinese standard GB/T 50081-2019 [29], the loading speed is established as 0.6 MPa/s. The test results and failure phenomenon are given in Table 2 and Figure 3, respectively.

Table 2. Compressive strength of concrete.

Concrete Type	C50-1	C40-1	C40-2
Compressive strength (MPa)	56.10	48.30	46.60

Figure 3. Failure phenomenon of cubic specimens.

2.2.2. Steel Bar

The designed strength grade of longitudinal reinforcement in the columns is HRB500 and the diameter is 20 mm. Meanwhile, the designed strength grade of the longitudinal reinforcement in the beam is HRB400 and the diameter is 16 mm. The strength grade of the stirrups used in the beam and columns is HPB300 and the diameter is 6 mm. According to the requirements of Chinese standard GB/T 228.1-2010 [30], a tensile strength test is carried out on the steel with a loading speed of 1.2 kN/s. The failure phenomenon and experimental data are given in Figure 4 and Table 3.

Figure 4. Failure phenomenon of steel reinforcement.

Table 3. Experimental results of steel reinforcement.

Steel Types	Diameter (mm)	Yield Strength (MPa)	Ultimate Strength (MPa)	Elongation Percentage (%)	Elastic Modulus (GPa)
HPB300	6	382	534	16.2	210
HRB400	16	464	634	32.9	206
HRB500	20	574	736	28.9	206

2.2.3. Steel Plate

The thickness of the steel plate wrapping the column is 10 mm, while the thickness values of the beams are 2 mm and 3 mm, respectively. The thickness of the steel plate used for manufacturing connectors are 3 mm and 5 mm, respectively. The failure phenomenon is given in Figure 5, and the mechanical properties of the steel plate are shown in Table 4.

Figure 5. Failure phenomenon of steel plates.

Table 4. Experimental results of steel plates.

Steel Type	Thickness (mm)	Yield Strength (MPa)	Ultimate Strength (MPa)	Elastic Modulus/GPa
Q345	2	346	459	206
Q345	3	420	503	206
Q345	5	333	444	206
Q345	10	359	425	206

2.3. Manufacturing of the Specimens

1. Pasting of the strain gauges. According to the stress characteristics of the joint, strain gauges are pasted on the longitudinal reinforcement, stirrups, and steel plates near the core area (Figure 6).

(**a**) (**b**) (**c**)

Figure 6. Pasting of the strain gauges: (**a**) longitudinal reinforcement; (**b**) hoop reinforcement; (**c**) steel plate.

2. Pouring the column concrete and wrapping the steel plate. For specimens JGJ1–JGJ3, after pouring and curing the column concrete (Figure 7a), the epoxy resin adhesive is applied on the concrete surface and the steel is wrapped. Then, the Π-shaped steel is welded onto the wrapped steel of the column. Finally, the longitudinal reinforcement of the beam is welded onto the flange of the connector, as shown in Figure 7b. The wrapped steel used for the column and the beam is formed by welding four steel plates together. All welding mentioned in this paper is carried out using arc welding, including the following two types of welding: welding between steel plates and steel bars. For the first type of welding, the calculated thickness of the weld seam is the thickness of the thinner plate at the welding site. For the second type of welding, the welding thickness cannot be less than 0.3 times the diameter of the steel bar, and the weld width cannot be less than 0.8 times the diameter of the steel bar [31].

(**a**) (**b**)

Figure 7. Manufacturing of the column: (**a**) pouring of the concrete; (**b**) connection of Π-shaped steel and the longitudinal bar of the beam.

3. Pouring the beam concrete and wrapping the steel plate. The process of pouring concrete is the same as that used for the column. The process of concrete pouring and

steel wrapping is shown in Figure 8a. Holes are then drilled, and the chemical anchor bolts are implanted (Figure 8b).

(**a**) (**b**)

Figure 8. Manufacturing of the beam: (**a**) pouring of the concrete; (**b**) arrangement of the chemical anchor bolts.

2.4. Loading of the Specimen

The test was carried out in the Shaanxi key laboratory to ensure the safety and durability of the concrete structures, and the test loading device is shown in Figure 9. The axial load is applied using a 2000 kN jack, while the lateral load is applied using a 500 kN hydraulic servo actuator, manufactured by MTS. Since the specimen is intercepted from the contraflexure point of the joint in the actual engineering structures, the hinged support is used to support the specimen. To ensure the free movement of the top of the column in the horizontal direction, a sliding support is set above the jack.

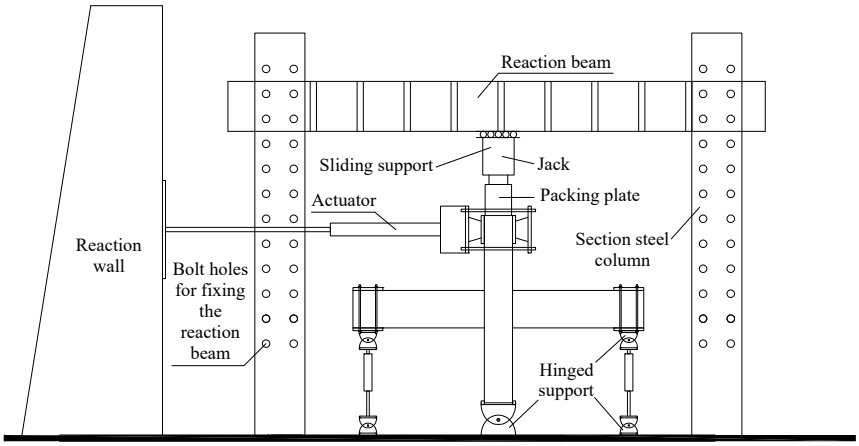

Figure 9. Loading device.

Before the loading process begins, a vertical load is applied on the top of the column and the stability of this load is maintained throughout the loading process. The horizontal load is then applied, and the loading direction is specified as positive in the push-out direction and negative in the pull-back direction.

The ratio of axial compression stress to strength is 0.19; thus, the value of vertical load to be applied is 400 kN. Based on the specifications of Chinese standard JGJ 101-2015 [32], the displacement control method is used for the loading. Before yielding the specimen, the displacement increment at each level is set to 3 mm, meaning that loading is cycled

once. When the specimen is yielded, each displacement increment is adjusted to 21/15 mm (21 mm for BZJ and 15 mm for JGJ, which meets the test demand based on the previous finite element simulation results), and the loading is cycled three times. The loading method is given in Figure 10.

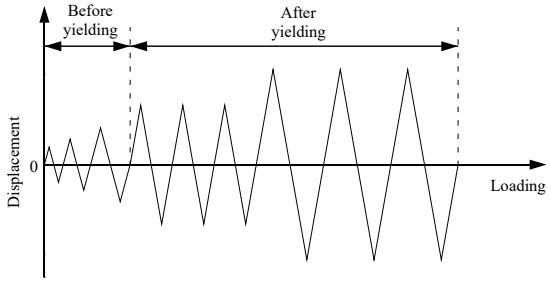

Figure 10. Loading system.

At the late stage of the loading, the specimen is demonstrably damaged if any of the following conditions are met: (1) in the core area, the crack width is significantly expanded or the steel plate is seriously deformed; (2) the overall deformation of the joint is large; (3) the bearing capacity is reduced to 85% of the maximum bearing capacity.

3. Failure Phenomenon and Analysis

3.1. Failure Phenomenon

1. BZJ

The failure phenomenon in the loading process of the specimen is given in Table 5, and the final damage phenomenon is shown in Figure 11.

Table 5. Experimental phenomenon of BZJ.

Displacement	Experimental Phenomenon
6 mm	Small deformations of the beam near the core area could be observed, and a vertical crack, 100 mm in length, was observed at the column ends.
9 mm	Two vertical cracks with lengths of 40 mm and 200 mm appeared at the beam end of the joint core area.
15 mm	Three new vertical cracks appeared at the end of the left beam of the joint core, while a vertical crack with a length of 200 mm and an oblique crack with a length of 220 mm appeared at the end of the right beam.
18 mm	Existing cracks increased in width and no new cracks appeared.
21 mm	One vertical crack with a length of 110 mm and one oblique crack with a length of 170 mm appeared at the right beam near the core area. The existing cracks at the column near the core area extended into an oblique crack, 50 mm in length.
	The specimen was yielded.
42 mm	One vertical crack, 100 mm in length, could be observed at the right beam end and one oblique crack, 180 mm in length, was observed at the left beam end.
63 mm	One vertical crack, 120 mm in length, could be observed at the left beam, which then developed obliquely to the right, extending up to the bottom of the beam. The concrete at the right beam end peeled off.
84 mm	The deformation of the right beam end further increased and the concrete on the upper surface spalled off. A penetrating crack formed at the left beam end and two straight oblique cracks at the top of the beam developed.
105 mm	The concrete cracks at the left beam end widened and the concrete spalled off on the lower surface. The stirrups, longitudinal bars, and strain gauge wires could be seen at the right beam due to the spalling off of the concrete.
126 mm	Two inclined cracks, two vertical cracks, and one horizontal crack were formed in the core area. The stirrups, longitudinal reinforcement, and strain gauge wires were exposed.
147 mm	The number of cracks on the beam continued to increase, and the spalling of the concrete became more severe. At this point, the bearing capacity was reduced to 85% of ultimate load, and it was determined that the specimen had been damaged.

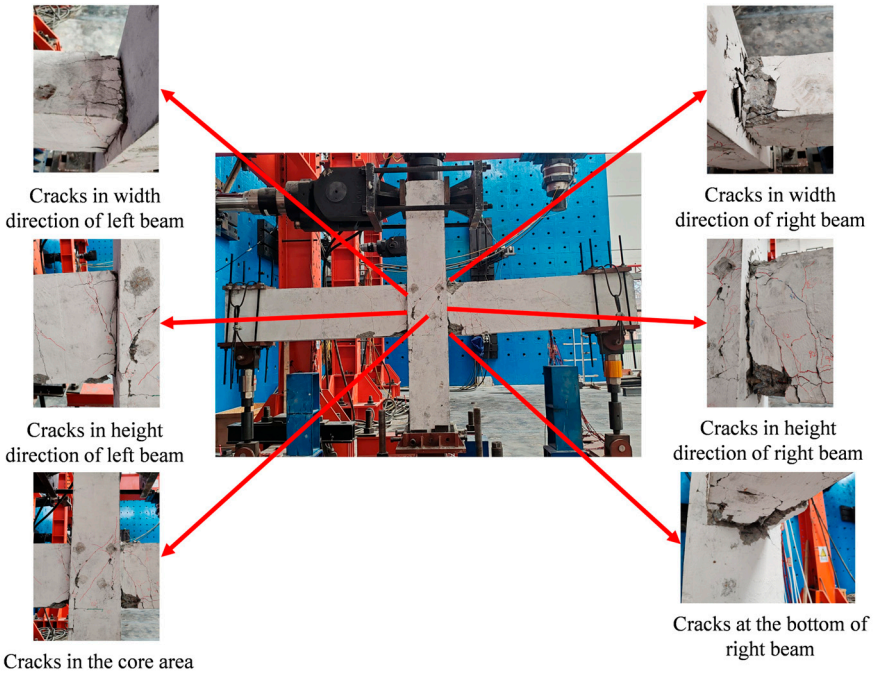

Figure 11. Failure phenomenon of BZJ.

2. JGJ-1

The failure phenomenon of the specimen when loaded is given in Table 6, and the final damage phenomenon can be observed in Figure 12.

Table 6. Experimental phenomenon of JGJ-1.

Displacement	Experimental Phenomenon
3–18 mm	There was no phenomenon that could be observed during this loading process.
21 mm	Smaller deformations were observed in the chemical anchor bolts attached to the core area.
24 mm	The sound of concrete deformation could be heard. One diagonal crack of 50 mm was observed in the concrete of beams.
	The specimen was yielded.
39 mm	New cracks appeared in the concrete of the left beam and existing cracks in the concrete of the right beam developed obliquely.
54 mm	Squeezing sounds of the steel plate deforming could be heard, accompanied by the sound of concrete deformation.
69 mm	The concrete of the right beam showed oblique and vertical cracks. Cracks in the concrete of the left beam developed at the top of the beam. The weld seam of the wrapped steel of the beam and column cracked along the height direction of the beams, with a length of 30 mm. The upper and lower surfaces of the left beam, as well as the lower surface of the right beam, exhibited bulging, caused by the deformation of the internal concrete.
84 mm	The cracks in the wrapped steel of the beams and columns continued to develop in the direction of the height and width of the beam. The chemical anchor bolts arranged on both sides of the column were squeezed to produce a small deformation.
99 mm	The length of the crack in the weld seam in the position of the beam–column connection was 75 mm along the height direction of the beam. The length of the cracks along the width direction of the beam was 100 mm. The crack length of the weld seam of the wrapped steel of the beam and column was 70 mm.
114 mm	Cracks appeared at the weld seam of the wrapped steel of the column, and the lengths of the cracks on the right and left sides were 130 mm and 100 mm, respectively.
129 mm	The concrete wrapped in steel was crushed. The wrapped steel of the upper surface of the beam and the column were completely disconnected, and the length of the weld cracks on the lower surface of the beam continued to increase.
144 mm	On the left side, the crack length of the weld seam of the steel plate wrapping the beam and column along the height direction of the beam was 90 mm, while the crack length of the weld on the right side was 80 mm. The crack length of the weld of the wrapped steel of the column was 310 mm, and the wrapped steel on both sides of the core area was detached from the concrete. At this point, the bearing capacity was reduced to 85% of the ultimate load, and it was determined that the specimen had been damaged.

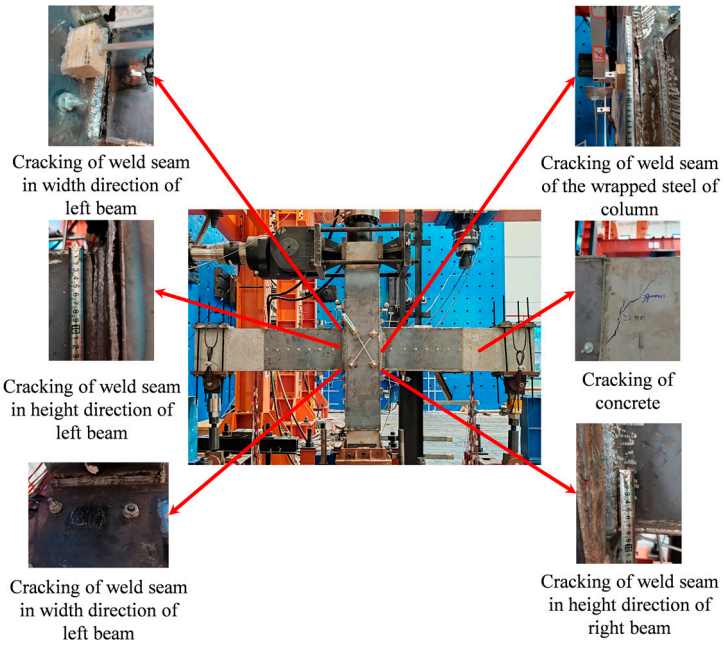

Figure 12. Failure phenomenon of JGJ-1.

3. JGJ-2

The failure phenomenon of the specimen when loaded is given in Table 7, and the final failure phenomenon can be seen in Figure 13.

Table 7. Experimental phenomenon of JGJ-2.

Displacement	Experimental Phenomenon
6–9 mm	The concrete inside the wrapped steel could be heard being squeezed, and no cracks appeared in the untreated concrete.
12 mm	The wrapped steel was squeezed and minor deformations of the chemical anchor bolts arranged on the columns could be observed.
15–18 mm	One crack in the weld seam in the position of the beam–column connection appeared in the height direction of the beam.
21 mm	One oblique crack, 120 mm in length, was observed in the concrete of the left beam. One oblique crack, 30 mm in length, was observed in the concrete of the right beam and developed toward the lower right side.
24 mm	Minor cracks appeared in the weld seam in the position of the beam–column connection.
39 mm	The wrapped steel on the upper surface of the beam appeared to be bulging and there were visible cracks at the welds of the encased steel of the column. One oblique crack with a length of 100 mm could be observed in the concrete of the left beam and developed to the upper left.
	The specimen was yielded.
54 mm	Weld seam cracks with a length of 10 mm appeared in the position of the beam–column connection along the height and width direction of the beam. Vertical cracks, 200 mm and 250 mm in length, appeared in the concrete of the beams.
69 mm	The wrapped steel of the beam was continuously squeezed, visibly increasing in height to about 10 mm.
84 mm	The weld seam of the wrapped steel made a large cracking sound, and the crack length of the weld between the wrapped steel of the beam and column was 20 mm.
99–114 mm	The concrete of the left beam showed one oblique crack developing downward to the left, with a length of 100 mm.
129 mm	One crack with a length of 500 mm appeared in the weld seam of the steel plate wrapping the column.
144 mm	The bolts used for fixing the encased steel of the column broke.
159 mm	The weld seam on the right side in the position of the beam–column connection cracked in the height direction of the beam by 120 mm, at which time the bearing capacity was reduced to 85% of the ultimate load, and it was determined that the specimen had been damaged.

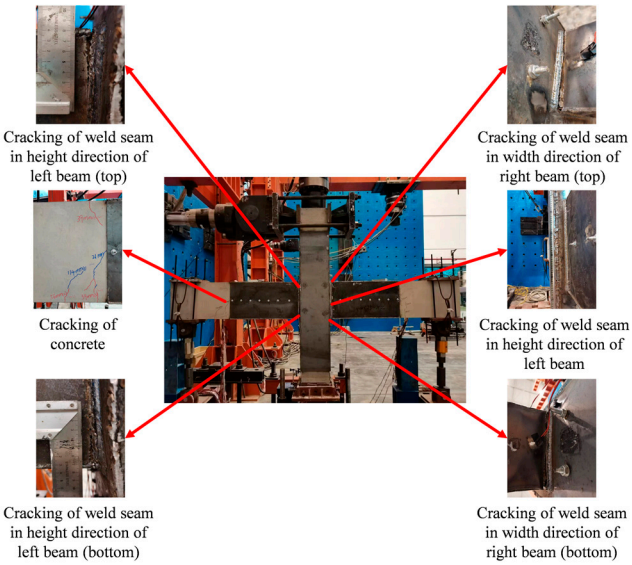

Figure 13. Failure phenomenon of JGJ-2.

4. JGJ-3

The damage process of the specimen when loaded is introduced in Table 8, and the final damage phenomenon is given in Figure 14.

Table 8. Experimental phenomenon of JGJ-3.

Displacement	Experimental Phenomenon
3–9 mm	There was no experimental phenomenon that could be observed during this loading stage.
12 mm	Minor deformation of the chemical anchor bolts arranged on the columns could be observed.
15 mm	One oblique crack, 250 mm in length, developed toward the lower left side of the concrete of the left beam. Two vertical cracks appeared on the concrete of the right beam.
18–24 mm	The sound of concrete and steel plates deforming by compression could be heard.
39 mm	The concrete of the left beam showed two oblique cracks with lengths of 200 mm and 50 mm, respectively. The existing crack in the concrete of the right beam extended to the bottom. Vertical cracks, 10 mm in length, were observed in the weld seam in the position of the beam–column connection.
	The specimen was yielded.
54–69 mm	The chemical anchor bolts arranged on the columns near the core area were squeezed by the steel plates and deformed severely. Cracks in the weld seam in the position of the beam–column connection continued to develop.
84 mm	The bulging of the wrapped steel of the specimen could be observed.
99 mm	The chemical anchor bolts attached to the column on the core area had failed.
114 mm	One crack with a length of 160 mm appeared at the weld seam of the wrapped steel of the column.
129 mm	The weld seam in the position of the beam–column connection was completely cracked on the upper and lower parts of the beam, and the length of the cracks was 140 mm. The length of the cracks in the welds of the wrapped steel of the column was 500 mm.
144 mm	The weld seam of the wrapped steel of the column was severely deformed and the bolts used to fix the steel plate of the column were broken. At this point, the bearing capacity was reduced to 85% of the maximum load, and it was determined that the specimen had been damaged.

5. Failure of the core area of JGJ1–JGJ3

To study the damage of the concrete and connector encased in steel plates in the core area, the outer steel near the core area was removed after the experiment.

The states of the concrete and the connector are shown in Figure 15. From the figure, it can be found that there is basically no damage to the beam concrete, indicating that the connection between the concrete, connector, and the wrapped steel of the column is still effective, and the damage is mainly caused by the cracking of the wrapped steel weld, which can be seen in Figure 15a. Due to the restraining effect of the encased steel, the concrete is basically intact in the core area, which is shown in Figure 15b. To ensure the integrity of the specimen, eight bolts are arranged on the encased concrete column. Before the joint failed, the bolts were all pulled off, and then, the cracking of the wrapped steel welds of the column occurred, which can be seen in Figure 15c. The connector sustained no significant deformation when the specimen was broken, and there are no crack at the weld joint connected to the wrapped steel, as shown in Figure 15d.

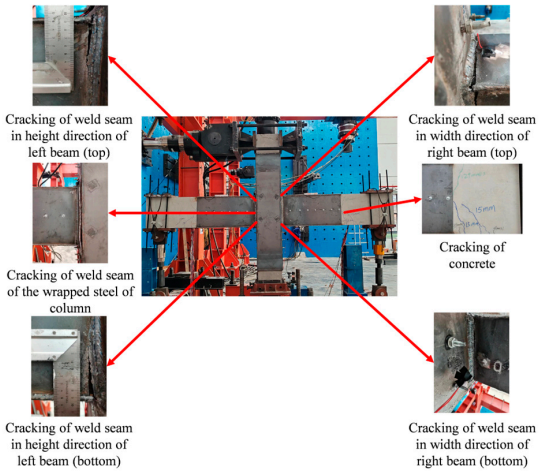

Figure 14. Failure phenomenon of JGJ-3.

Figure 15. Failure phenomenon of the core area: (**a**) concrete of the beam near the core area; (**b**) concrete in the core area; (**c**) cross-section of bolts after the test; (**d**) experimental phenomenon of the connector.

3.2. Failure Process Analysis

(1) The cracks of BZJ mainly appear in the core area. When the joint is damaged, the deformation of the beam is large, and the longitudinal reinforcement of the beam is exposed after the spalling off of the concrete. While the cracks of JGJ1–JGJ3 mainly appear in the wrapped steel welds of the beam and the column near the core area, the concrete is basically intact due to the restraint effect of the wrapped steel. These phenomena indicate that after the specimen has been treated with wrapped steel, the main stress components of the joint specimen change. The bearing capacity of BZJ mainly relies on the stress of the steel reinforcement and compression of the concrete, and when these two materials are damaged or reach the yield state, the component is damaged. Meanwhile the new type of joint specimen mainly relies on the stress of the wrapped steel; thus, the bearing capacity is higher before the welds of the wrapped steel fail.
(2) Compared with JGJ2, JGJ3 has a larger loading displacement when the weld cracks of wrapped steel appear, indicating that increasing the thickness of the wrapped steel of the beam can delay the time the cracks take to appear and enhance the integrity of the joint.
(3) Compared with JGJ3, JGJ1 has a larger cracking displacement before the weld seam cracks, showing that the deformation capacity is stronger when the connector thickness is smaller.

Based on the descriptions of the previous images and text, as well as the design intention of this paper, the weak link of the new type of specimen is the beam, specifically, the beam end near the core area, which is subjected to significant bending moments. Before yielding the steel and weld seams, the bending moment is mainly borne by both parties. By ensuring the quality of the weld seam, the specimen should first exhibit the yielding of the steel plate, though in the actual loading process, the steel plate does not yield, and the weld seam is damaged. After the weld seam cracks, the longitudinal bars of the beam begin to bear the load and transmit this part of the load to the wrapped steel of the column through the connector. As the load increases, the weld seam of the wrapped steel of the column cracks, resulting in a decrease in the stress performance of the specimen. At the same time, the thicker the steel plate of the beam, the easier it is to ensure the quality of the weld, as thinner steel plates are prone to penetration under high temperatures, affecting the quality of the welding. Therefore, the mechanical properties of the specimen are affected by the thickness of the beam's steel and the quality of the weld seam.

4. Result Analysis of Testing

4.1. Hysteretic Curve

A hysteretic curve is a graphical representation of the load–displacement relationship of a structure or member under the influence of cyclic loading. The hysteretic curve reflects the deformation properties, stiffness variation, and energy dissipation capacity of the specimen. The following results can be obtained from Figure 16:

(1) At the early stage of the test, hysteretic curves are basically straight, indicating that the specimen has sustained no damage.
(2) As the loading displacement increases, the hysteretic curve gradually becomes fuller, and the slope gradually becomes smaller, indicating that the specimen is damaged during the loading process, resulting in a gradual increase in its energy dissipation capacity and a decrease in its stiffness.
(3) The hysteretic curve of BZJ is Z-shaped, while those of JGJ1–JGJ3 are inverted S-shaped. This is because the damage to the cast-in-place specimen is more serious

during the loading process, which leads to the hysteretic curve showing a larger slip section and a poorer energy dissipation capacity. Meanwhile, the main stressing parts of the new types of joints are the wrapped steel and weld seam, which also show certain slip characteristics, though the shape of curve is still full.

(4) The curves of the new types of joints have the same shape. Compared with JGJ3, the hysteretic curve of JGJ2 exhibits a more pronounced pinching phenomenon, which indicates that increasing the thickness of the wrapped steel and Π-shape steel can enhance the mechanical performance of the component and can consume more energy in the loading process.

(5) From the hysteresis curves of the four specimens, it can be seen that the loading displacements corresponding to the maximum bearing capacity of BZJ, JGJ1, JGJ2, and JGJ3 are 84 mm, 39 mm, 39 mm, and 39 mm, respectively. This indicates that the stiffness of the specimens increases significantly with the reinforcement of wrapped steel, and significant damage occurs at smaller loading displacements. After reaching the maximum bearing capacity, BZJ meets the failure criteria after two cycles of loading, while JGJ1–JGJ3 fail after seven cycles of loading, indicating that wrapped steel reinforcement is effective in increasing the deformation and energy dissipation capacity of the specimen.

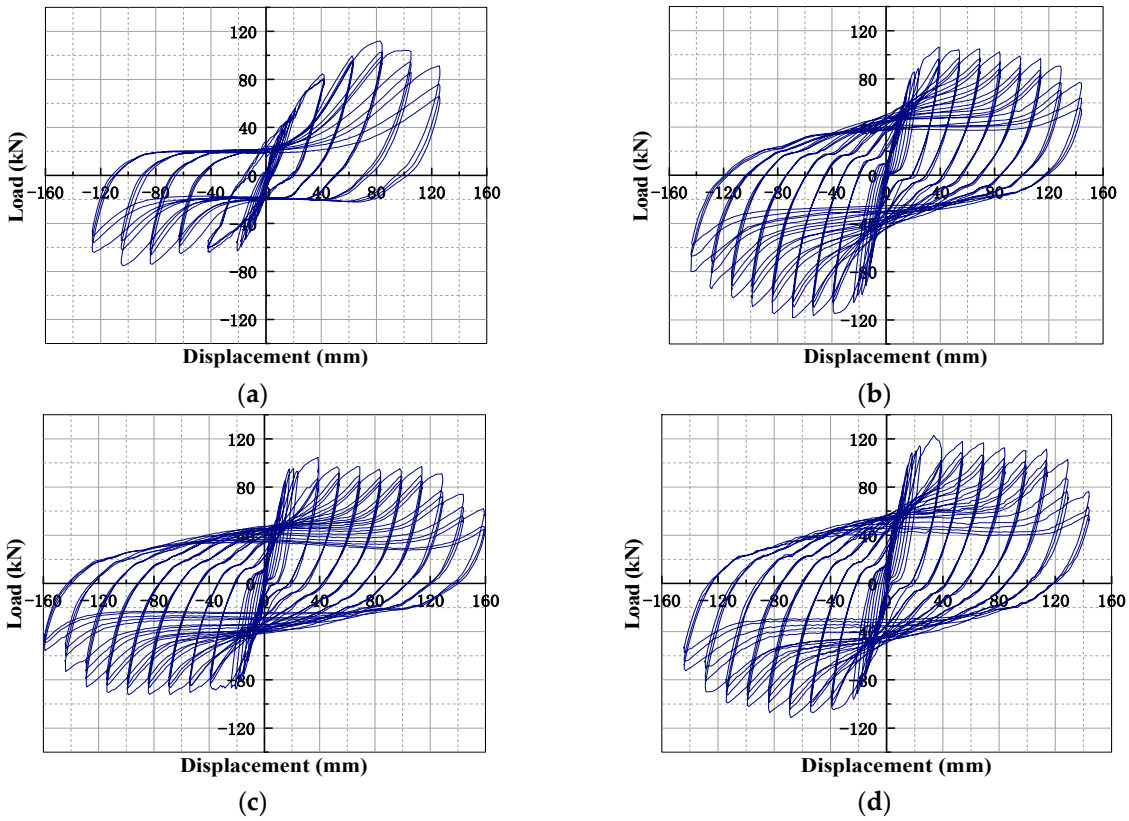

Figure 16. The hysteretic curves of specimens (**a**) BZJ; (**b**) JGJ1; (**c**) JGJ2; (**d**) JGJ3.

4.2. Skeleton Curve

This curve is an envelope connected by the ultimate load points of the hysteretic curve, reflecting the limits of the structure during cyclic loading. By studying the skeleton curve, the seismic performance of the structure can be better evaluated, providing the theoretical basis for engineering practices. The skeleton curve is given in Figure 17, and the different characteristic load values are shown in Table 9. The following be concluded from the comparative analysis of the test results:

(1) The skeleton curve of BZJ is basically straight in the preloading phase, and the specimen sustains no serious damage, although some cracks have appeared on the concrete of the beam. With gradual accumulation of damage, the growth trend of the curve begins to slow down and decline after reaching the maximum bearing capacity.

(2) The skeleton curves of JGJ1–JGJ3 are also basically straight in the early stage of the experiment, and at this time, the cracks of the specimen mainly appear on the concrete of the beam without wrapped steel, indicating that the joint has sustained little damage. Then, the weld seam of the wrapped steel begins to crack, decreasing the rate at which the curve increases. After reaching the maximum bearing capacity, the curve begins to decrease, but the decreasing trend is slower than that of BZJ, which indicates that the wrapped steel treatment improves the stress properties of the specimen.

(3) Comparing the skeleton curves of JGJ1 and JGJ3, it can be obtained that the stiffness of the two specimens is basically the same at the beginning of the test, and the maximum load is 106.4 kN and 122.9 kN, respectively. Then, the carrying capacity decreases slowly. Through the strain gauges arranged on the connectors, it can be found that the strain values of the connectors of all the new type of joints are very small, indicating that the influence of the connectors on the bearing capacity is very small, and the difference in bearing capacity is perhaps due to the poor quality of the weld seam.

(4) Through the comparison of JGJ2 and JGJ3, it is concluded that the stiffness remains basically unchanged when no damage or less damage occurs. The skeleton curves increase linearly, and the carrying capacity decreases slowly when the specimen has reached the maximum bearing capacity. The bearing capacities of JGJ2 and JGJ3 are 104.8 kN and 122.9 kN, respectively, which indicates that the influence of the thickness of the wrapped steel on the bearing capacity is significant.

(5) Comparing the characteristic load of the joint, it can be found that the characteristic load values of the specimens treated with a steel plate are higher than those of the standard joint. By comparing and analyzing the test results of the new types of specimens, it can be found that JGJ3 has the highest characteristic load values, indicating that the influence of the thickness of the wrapped steel is relatively significant. At the same time, it can also be demonstrated that the greater the amount of steel used, the more obvious the effect of improving the seismic performance becomes.

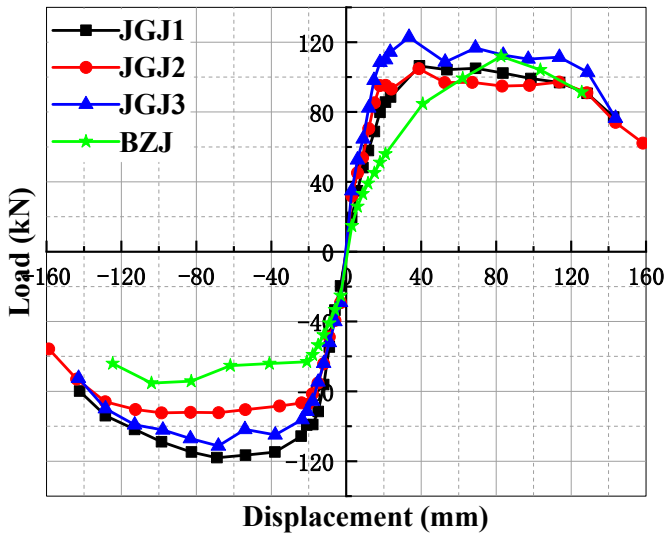

Figure 17. Skeleton curves of the specimens.

Table 9. The load values at different stages.

Number	Direction	Yield Load (kN)	Maximum Load (kN)	Ultimate Load (kN)
BZJ	Push	86.49	111.95	91.31
	Pull	63.73	75.29	64.07
JGJ1	Push	88.30	106.38	77.13
	Pull	100.56	118.02	100.32
JGJ2	Push	93.25	104.80	89.08
	Pull	79.54	92.30	78.46
JGJ3	Push	106.78	122.90	104.47
	Pull	90.90	111.30	94.61

4.3. Ductility Analysis

The ductility coefficients of this test are given in Figure 18. Considering the variability of the ductility in the push and pull directions, the average values are selected for analysis.

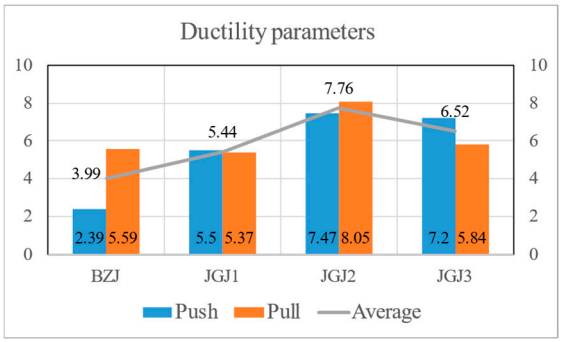

Figure 18. Ductility parameters of the specimens.

(1) Compared with BZJ, the ductility coefficients of JGJ1–JGJ3 increase by 36.3%, 94.5%, and 63.4%, respectively, indicating that the wrapped steel plates restrain the formation and development of cracks in the internal reinforced concrete part, and the good mechanical properties of the steel plates themselves ensure that the specimens have a good elasticity-plasticity deformation capacity. After reaching the maximum bearing capacity, the specimen can still maintain a certain load capacity.

(2) Compared with JGJ1, the ductility coefficient of JGJ3 increases by 19.9%, which indicates that increasing the connector thickness could significantly enhance the integrality of the specimen and maintain the effectiveness of the connection after the destruction of the wrapped steel weld, thus enhancing ductility.

(3) The coefficient of JGJ2 increases by 19.0% compared to that of JGJ3, which indicates that the wrapped steel thickness of the beam has an adverse effect on the ductility. This may be due to the fact that as the thickness of the steel plate increases, it shares more load at the beginning of the experiment and its bearing capacity decreases faster after the weld cracks. At the same time, the greater the wrapped steel thickness, the stronger the restraining effect on the RC part, resulting in the smaller plastic deformation of the concrete when it reaches the limit state, which leads to a reduction in ductility.

4.4. Rigidity Degeneration

Rigidity degeneration refers to the rigidity (i.e., the ability to resist deformation) of a structure or material that gradually decreases with time or the number of loadings,

especially under repeated or cyclic loading. The rigidity degeneration curve of this test is given in Figure 19. Through the analysis of the test results, the following can be concluded:

(1) By comparing the rigidity degeneration curves of BZJ and JGJ1–JGJ3, it can be seen that the initial stiffness of the standard joint is smaller than that of the new types of joints. As the experiment progresses, the stiffness of both specimens starts to decrease after the damage of the specimens occurs. For BZJ, stiffness decreases, mainly due to the failure of the concrete, increasing the stress in the steel bars; while for JGJ1–JGJ3, the stiffness decreases mainly due to the cracking of the steel plate welds. The stiffness degeneration of the new types of joints is relatively fast because the welds are mainly damaged under tension. The stiffness degeneration rates of the two types of specimens are basically the same when the specimens are close to damage.

(2) The rigidity of the new types of joints at the time of failure is basically the same as that of the cast-in-place specimen, indicating that the wrapped steel treatment can maintain a certain stiffness during failure while significantly enhancing the initial stiffness of the specimen. This is beneficial for the structure, helping with maintaining integrity after experiencing external loads.

(3) Compared with JGJ3, the initial stiffness of JGJ1 is smaller, but the stiffness decreases at a slower rate, which is mainly due to the existence of certain defects in the welds of JGJ1. After the cracks of the wrapped steel welds appear at the early stage of loading, the main force part becomes the wrapped steel of the column, ultimately leading to the cracking of the wrapped steel welds. Considering that the stresses in the Π-shaped steel plate are small throughout the test, the effects of the thickness of the connector is not significant.

(4) The initial stiffnesses of JGJ2 and JGJ3 are basically the same, and both drop rapidly at the beginning of loading. Compared with JGJ3, the drop of JGJ2 is larger, but the drop rate of the two specimens is consistent when the displacement is 25 mm. This is mainly due to the fact that an increase in the wrapped steel thickness of the beam increases the constraint effect on the concrete, which can effectively improve the initial stiffness. However, the effect of the thickness of the wrapped steel gradually decreases with the development of cracks in the weld seam.

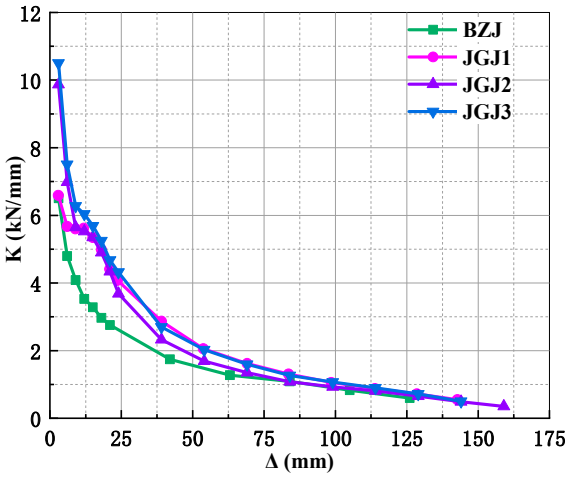

Figure 19. Rigidity degeneration of the specimens.

4.5. Energy Dissipation Capacity

This capacity refers to a specimen's ability to absorb and dissipate input energy through plastic deformation mechanisms under external loading. The cumulative energy dissipation curves are given in Figure 20, from which the following can be observed:

(1) Compared with JGJ1–JGJ3, the energy dissipation capacity of BZJ is obviously weaker, which is due to the fact that the main bearing materials of the cast-in-place specimen are steel reinforcement and concrete, and the concrete is subjected to tensile and compressive effects under cyclic loads, which results in rapid destruction, leading to the lower energy dissipation capacity. The load of JGJ1–JGJ3 is mainly borne by the wrapped steel, and due to the good mechanical properties of the steel plate, a large amount of energy is consumed during the deformation process, so the new type of joint has a better energy dissipation capacity.

(2) Compared with JGJ3, the energy dissipation capacities of JGJ1 and JGJ2 are relatively poor, and the gap between the cumulative energy dissipation curves of JGJ1 and JGJ2 and those of JGJ3 gradually becomes bigger with the increase in loading displacement. This shows that increasing the amount of steel can effectively improve the energy dissipation capacity but has little effect on the damage deformation.

(3) The cumulative energy dissipation curves of JGJ1 and JGJ2 are basically the same. During the gradual increase in elastic-plastic deformation, the cumulative energy dissipation curve of JGJ1 is slightly larger than that of JGJ2, but the value of the two specimens is basically the same when they reach the destructive load. This may be due to the fact that the wrapped steel thickness of the beam of JGJ1 is larger than that of JGJ2, which results in more energy being consumed before the specimen is damaged. However, when the specimen is damaged, there is not much difference in the energy dissipation capacity of JGJ1 and JGJ2 because the connecting parts begin to experience stress.

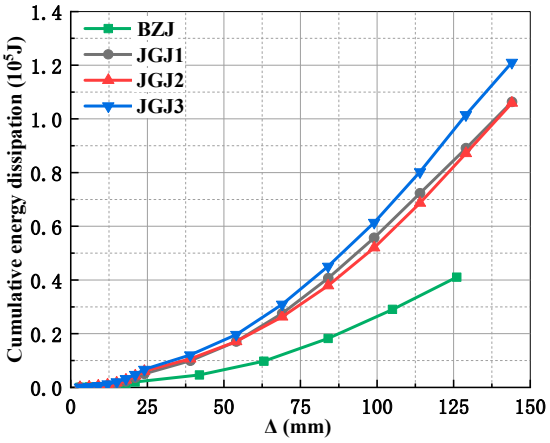

Figure 20. Cumulative energy dissipation of the specimens.

The test results of this paper are similar to those of [16,17]. After the reinforcement treatment, the steel plate bears most of the load and restrains the deformation of the concrete before yielding, and the mechanical properties of steel are much better than those of concrete. Therefore, wrapped steel can significantly improve the seismic performance of the structure. However, compared with the investigation of [16], the seismic performance improvement of the specimen in this paper after the treatment with wrapped steel is not so obvious, which is mainly because the steel haunches in [16] can bear the load the bolted wrapped steel yields, so its performance is better.

5. Conclusions

This paper focuses on the experimental study of the seismic properties of a new type of joint. The beam and column are wrapped by a steel plate and connected through the Π-shaped steel plates that were welded on the encased steel of the column. The wrapped

steel thickness of the beam and the Π-shaped steel plate are used as testing variables for the specimens. The differences between the mechanical properties of this new type of joint and the standard joint are analyzed through the cyclic horizontal loading experiment, and the influence of different factors on the seismic performance of the specimens are investigated.

(1) The failure of BZJ mainly appears in the core area of the joint. With the increase in loading displacement, the concrete is gradually destroyed, and the longitudinal reinforcement yields. The damage of JGJ1–JGJ3 firstly appears in the connection welds of the beam and column cladding steel. Then, cracks appear in the weld of the column cladding steel. When the joint fails, the wrapped steel weld seam of the column within the range of the beam height cracks. This shows that the force transfer mechanism of the specimen after steel cladding treatment has changed, and there is a change from reinforced concrete force to wrapped steel force.

(2) Compared with BZJ, the carrying capacity of JGJ1–JGJ3 increases by −5.0%, −6.4%, and 9.8%, respectively, indicating that the effectiveness of the new type of joint in bearing capacity enhancement needs to be further investigated. Through the analysis of the failure phenomenon, the bearing capacity of JGJ1–JGJ3 is primarily affected by the quality of the weld seam. All loading displacements of the new type of joint when reaching the damage criterion are larger than the corresponding values of the standard specimens, indicating that the good deformation capacity of wrapped steel enhances the deformation capacity of the joint.

(3) The stiffness of all the joints gradually decreases as loading progresses. Considering that the cracking of JGJ1–JGJ3 is mainly due to the fracture of the weld seam, their stiffness decreases faster than that of the standard specimens, and the larger the amount of steel plate used, the faster the stiffness degeneration. When the specimens reached the damage state, the stressed parts of all specimens become reinforced concrete, so the stiffness values are basically the same.

(4) Following the wrapping steel treatment, the energy dissipation capacity increases significantly, and the cumulative energy dissipation of JGJ3 with the best mechanical properties is three times that of BZJ, indicating that the seismic properties of the joint are effectively enhanced through the wrapping steel treatment.

(5) By analyzing the seismic performance of JGJ1–JGJ3, it can be found that the thickness of the wrapped steel of the beam enhances the mechanical performance of the specimen more obviously, while the role of the Π-shaped steel plate is not obvious. This is due to the fact that the wrapped steel is the main force part. The specimen has already reached the damage state after the connecting weld has penetrated through the wrapped steel, and the effect of the connector is not obvious.

The experimental results indicate that the quality of the weld seam has a significant impact on the mechanical properties of the specimen. Therefore, when using the reinforcement method proposed in this paper to treat the structure, it is essential to ensure the quality of the weld seam. If the quality of the weld cannot be guaranteed, reinforcement measures should be taken at the location of the connection of the wrapped steel and the column to enhance the overall integrity of the structure.

At the same time, only the influence of steel plate thickness is considered, and the influence of the beam and column dimensions, material strength, and other factors on seismic performance is not studied. In a later stage, experimental research in this field will be carried out to promote the popularization and application of this type of reinforcement and renovation method in practical engineering.

Author Contributions: Conceptualization, J.W. (Jian Wu) and W.D.; methodology, J.Z.; software, L.H.; validation, Y.J., L.H. and J.W. (Jianhui Wang); formal analysis, Y.J.; investigation, L.H.; resources, J.W. (Jian Wu); data curation, J.W. (Jianhui Wang); writing—original draft preparation, Y.J.; writing—review and editing, J.W. (Jian Wu); visualization, W.D.; supervision, J.W. (Jian Wu); project administration, J.W. (Jian Wu); funding acquisition, J.Z. All authors have read and agreed to the published version of the manuscript.

Funding: This research was funded by the Shaanxi Provincial Department of Education Government-Enterprise Joint Funding Project (22JE017) and the Scientific Research Foundation for High-level Talents (XJ17T08).

Data Availability Statement: The original contributions presented in the study are included in the article, further inquiries can be directed to the corresponding author.

Acknowledgments: The authors would like to thank the Shaanxi Key Laboratory of Safety and Durability of Concrete Structures for the project testing.

Conflicts of Interest: Author Jian Zhou was employed by the company Northwest Engineering Corporation Limited. The remaining authors declare that the research was conducted in the absence of any commercial or financial relationships that could be construed as a potential conflict of interest.

References

1. Aycardi, L.E.; Mander, J.B.; Reinhorn, A.M. Seismic resistance of reinforced-concrete frame structures designed only for gravity loads-experimental performance of subassemblages. *ACI Struct. J.* **1994**, *91*, 552–563.
2. Kalogeropoulos, G.I.; Tsonos, A.D.G.; Konstandinidis, D.; Tsetines, S. Pre-earthquake and post-earthquake retrofitting of poorly detailed exterior, RC beam-to-column joints. *Eng. Struct.* **2016**, *109*, 1–15. [CrossRef]
3. Yavari, S.; Elwood, K.J.; Wu, C.L.; Lin, S.H.; Hwang, S.J.; Moehle, J.P. Shaking table tests on reinforced concrete frames without seismic detailing. *ACI Struct. J.* **2013**, *110*, 1001–1011.
4. *ACT-40*; Seismic Evaluation and Retrofit of Concrete Buildings. Applied Technology Council: Redwood City, CA, USA, 1996.
5. Chen, H.; Xie, Q.C.; Dai, B.Y.; Zhang, H.Y.; Chen, H.F. Seismic damage to structures in the, Ms 6.5 Ludian earthquake. *Earthq. Eng. Eng. Vib.* **2016**, *15*, 173–186. [CrossRef]
6. Huang, C.C.; Hsiao, H.J.; Shao, Y.; Yen, C.H. A comparative study on the seismic performance of, RC beam-column joints retrofitted by, ECC, FRP, and concrete jacketing methods. *J. Build. Eng.* **2023**, *64*, 105691. [CrossRef]
7. Tong, L.W.; Wang, T.T.; Xu, X.M.; Gao, F.; Shi, W.Z.; Zhou, F. Experimental study on, CFRP reinforcement and static performance of, CHS KT-joints. *J. Constr. Steel Res.* **2024**, *216*, 108618. [CrossRef]
8. Biddah, A.; Ghobarah, A.; Aziz, T.S. Upgrading of, Nonductile, Reinforced, Concrete, Frame, Connections. *J. Struct. Eng. ASCE* **1997**, *123*, 1001. [CrossRef]
9. Li, W.; Xu, L.F.; Qian, W.W. Seismic performance of 3-D steel beam to concrete-encased, CFST column joints: Tests. *Eng. Struct.* **2021**, *232*, 111793. [CrossRef]
10. Zhou, J.; Chen, Z.P.; Xu, W.S.; Liao, H.Y.; Wang, N. Seismic behavior of 3-D beam to, L-shaped concrete encased steel composite column joint: An experimental study. *J. Build. Eng.* **2022**, *52*, 104437. [CrossRef]
11. Lee, H.J.; Park, H.G. Seismic behavior of precast concrete beam-column joints with encased steel tube. *J. Build. Eng.* **2022**, *61*, 105296. [CrossRef]
12. Derakhshesh, P.; Mirghaderi, S.R.; Nouri, G.; Farzam, M. Behavior of new hybrid connection between steel beam and concrete-encased composite column. *J. Constr. Steel Res.* **2023**, *210*, 108043. [CrossRef]
13. Liu, X.C.; Meng, K.; Chen, X.S.; Zhang, J.; Cui, Y. Axial compression behavior of prefabricated, L-section thin concrete encased steel short columns. *J. Constr. Steel Res.* **2023**, *208*, 107989. [CrossRef]
14. Fang, J.P.; Zhou, L.Y.; Liu, J.H. Axial and eccentric compressive behavior of partially encased channel–concrete composite columns with bolted connections in modular buildings. *J. Build. Eng.* **2024**, *98*, 111173. [CrossRef]
15. Chen, G.X.; Gan, T.; Gao, X.L. Flexural behavior of, UHPC encased steel composite beams: Experiment and numerical simulation. *J. Constr. Steel Res.* **2025**, *226*, 109233. [CrossRef]
16. Cai, Z.W.; Liu, X.; Li, L.Z.; Lu, Z.D.; Chen, Y. Seismic performance of, RC beam-column-slab joints strengthened with steel haunch system. *J. Build. Eng.* **2021**, *44*, 103250. [CrossRef]
17. Zhang, X.G.; Yang, K.Y.; Hu, Q.M.; Wang, C.; Zhuang, L.D. Study of, U-shape steel-encased composite beams with variable sections under negative bending moments. *Structures* **2023**, *57*, 105098. [CrossRef]

18. Nguyen, V.P.; Nguyen, Q.H.; Couchaux, M.; Aribert, H.M.; Hjiaj, M. Hybrid steel beam to exterior, RC column joints with encased steel profile. *Eng. Struct.* **2024**, *306*, 117624. [CrossRef]
19. Ertas, O.; Ozden, S.; Özturan, T. Ductile connections in precast concrete moment resisting frames. *PCI J.* **2006**, *51*, 66–76. [CrossRef]
20. Choi, H.K.; Choi, Y.C.; Choi, C.S. Development and testing of precast concrete beam-to-column connections. *Eng. Struct.* **2013**, *56*, 1820–1835. [CrossRef]
21. Ali, A.Y.; AI-Rammahi, A.A. Flexural behavior of hybrid-reinforced concrete exterior beam-column joints under static and cyclic loads. *Fibers* **2019**, *7*, 94. [CrossRef]
22. Kurosawa, R.; Sakata, H.; Qu, Z.; Suyama, T. Precast prestressed concrete frames for seismically retrofitting existing, RC frames. *Eng. Struct.* **2019**, *184*, 345–354. [CrossRef]
23. Zhang, A.L.; Qiu, P.; Guo, K.; Jiang, Z.Q.; Wu, L.; Liu, S.C. Experimental study of earthquake-resilient end-plate type prefabricated steel frame beam-column joint. *Eng. Struct.* **2020**, *166*, 105927. [CrossRef]
24. Cao, W.L.; Yang, Z.Y.; Wang, X.J.; Dong, H.Y. Seismic behavior of prefabricated beam-column joint with π-shaped connector. *Structures* **2023**, *58*, 105553. [CrossRef]
25. Jannesari, Z.; Tasnimi, A.A. Investigating seismic behavior of a modified widened flange beam-column connection in, SMRF utilizing experimental, numerical and hybrid simulation. *J. Constr. Steel. Res.* **2023**, *207*, 107971. [CrossRef]
26. Joshi, M.K.; Murty, C.V.R.; Jaisingh, M.P. Cyclic behaviour of precast, RC connections. *Indian Concrete J.* **2005**, *79*, 43–50.
27. Huang, H.; Zhao, M.; Yang, B.X.; Huang, M.; Li, M. Research on seismic performance of replaceable prefabricated, RC beam-column joints. *Structures* **2024**, *65*, 106742. [CrossRef]
28. *GB 50205-2001*; Code for Acceptance of Construction Quality of Steel Structures. China Construction Industry Press: Beijing, China, 2001.
29. *GB/T 50081-2019*; Standard for Test Methods of Concrete Physical and Mechanical Properties. China Construction Industry Press: Beijing, China, 2019.
30. *GB/T 228.1-2010*; Metallic, Materials-Tensile testing-Part 1: Method of Test at Room Temperature. China Construction Industry Press: Beijing, China, 2010.
31. *GB 50661-2011*; Code for Welding of Steel Structures. China Construction Industry Press: Beijing, China, 2011.
32. *JGJ/T 101-2015*; Specification for Seismic Test of Buildings. China Construction Industry Press: Beijing, China, 2015.